This is an Author's Accepted Manuscript of an article published in Bioprocess and Biosystems Engineering (2013) 36:517-530. The final publication is available at Springer via http://dx.doi.org/10.1007/s00449-012-0807-0

Accelerating animal cell growth in perfusion mode by multivariable control: Simulation studies

Mihaela Sbarciog, Ines Saraiva and Alain Vande Wouwer

University of Mons, Automatic Control Laboratory, 31 Boulevard Dolez, 7000 Mons, Belgium
Tel.: +32-65374141
MihaelaIuliana.Sbarciog@Umons.ac.be
Ines.Saraiva@Umons.ac.be
Alain.VandeWouwer@Umons.ac.be

Abstract

This study considers the problem of manipulating in an optimal way the perfusion and bleed flow rates of a continuous culture of hybridoma cells, so as to achieve a fast transient start-up and reject potential disturbances. The proposed solution makes use of an analysis of the properties of the steady state solutions of the nonlinear dynamic model of the cell culture, and in particular the relationship between the two main limiting substrates, glucose and glutamine. The solution is implemented using extended prediction self-adaptive control. Simulation results demonstrate the approach potentiality.

***Keywords*—** model predictive control, optimization, bioprocess, hybridoma

1 Introduction

Recently, complex biomolecules have achieved eminent results in the treatment of several diseases such as diabetes, arthritis, multiple sclerosis, cancer, anaemia and HIV [1]. These high value biomolecules, such as certain vaccines, recombinant proteins and antibodies, are used with very target-specific functions, which led to a raise in their demands. Besides their diagnostic and therapeutics importance, they also present numerous opportunities for research [2]. However, their production is technologically complex and in some cases the only useful in vitro

process available is the cultivation of mammalian cells that are programmed to synthesize them. Hybridoma and CHO cells have become standards in the animal cell industry [3, 4].

Many animal cells can be grown as suspension in stirred tank reactors, which appear to be the most common practice in industry for large production of high value protein products [5]. The efforts for increasing the culture productivity in these systems focus on controlling the media on one hand, and the modes of providing it on the other hand. The most popular operating modes in animal cell culture are batch, fed-batch and perfusion modes [5, 6]. Batch and fed-batch modes do not offer many alternatives for control, as in these cases the feeding rate is either absent or restrained and the growth is inhibited by the accumulation of toxic metabolites, which cannot be removed. In perfusion mode, fresh medium is sent through the reactor to replenish the consumed nutrients, while an equal volume of spent medium is continuously withdrawn from it, allowing for the removal of toxic components. Cells are retained or recycled back to the reactor by some type of retention device. Higher cell concentrations and higher productivity are achieved in perfusion cultures than in conventional batch cultures [6].

Perfusion processes provide consistent culture conditions, high productivity and low product residence times. However, a successful perfusion culture requires tight control of the perfusion rate. Too low perfusion rates may result in nutrient limitation, accumulation of inhibitory metabolites and retardation in cell growth rate. Too high perfusion rates may result in wash out of the cells in perfusion cultures with partial cell retention. Perfusion cultures with complete cell retention are similar to batch cultures from cells growth perspective, as no steady state is reached until nutrient limitation occurs. However, mammalian cells do not grow below a certain minimal growth rate [8]. When cells are forced to grow below this rate the death rate increases. Thus, part of the cells start dying and the other cells maintain the minimal growth rate. Furthermore, since dead cells are also retained this results in a continuous increase of dead cells [7, 8, 9, 10]. Consequently, the addition of a small cell-containing flow (the bleed) out of the reactor is necessary for maintaining the viability of the culture, as well as for reaching steady state operation [7, 8, 11]. In spite of the wide acknowledgment of its necessity, the bleed flow is not used to improve the culture productivity. As [12] points out, not much is known on how to set its value, although studies on the open loop effects of this stream exist. Even less is known about the possibility of using it for the control and optimization of animal cell cultures. [12, 13] have conducted such a study for a simple model and presented an adaptive backstepping strategy which uses the perfusion and bleed rates to simultaneously control the cell and metabolite concentrations.

This paper is focused on using both perfusion and bleed rates for the control of an animal cell culture. This is a simulation study based on one of the widely used

models for animal cells growth, with the main goal of evaluating the difficulties arising in controlling such processes and identifying simple solutions that could be easily implemented in practice. This expertise will be used later on for the on-line control of our cells growth system, for which we are presently identifying a model.

The problem is formulated in the framework of multivariable predictive control, with the goal of regulating the amount of cells and the concentration of nutrients at arbitrary steady state values. The emphasis is on the fast growth of cells while decreasing the concentration of nutrients leaving the reactor. Two approaches are investigated: the first one considers the minimization of the squares of the total control error, the second one minimizes the squares of the control error for each system output. It is shown that the performance of the controlled system may be improved in the second approach by incorporating knowledge of the system dynamics in the cost index used for optimization.

2 Predictive Control

Nowadays, MPC (Model Predictive Control) is not just the name of some specific computer control algorithms, but the name of a specific philosophy in controller design, from which many kinds of computer control algorithms can be derived for different systems [14]. One of the important characteristics for the successful use of MPC in advanced industrial applications is its ability to take into account constraints imposed on both process inputs (manipulated variables) and outputs (controlled variables), constraints which usually affect quality, economic efficiency and safety. Moreover, MPC techniques allow to address in a direct way the multivariable nature of the processes, the extension from single input single output to multiple inputs multiple outputs (MIMO) systems being straightforward.

2.1 General principles of MPC

The key elements of MPC are [15]: the model used for prediction, the online optimization and the feedback compensation for model mismatch. There are no special demands on the form of model, the computational tool for online optimization and the form of feedback compensation [14]. The block diagram of the MPC control loop is illustrated in Figure 1 and the working principle is as follows: An appropriate model is used to predict the process output, $y(t+k/t)$, $k = 1,\ldots,N_p$ over a future time interval known as prediction horizon, N_p. A sequence of control actions, $u(t+j/t)$, $j = 0,\ldots N_u-1$ over the control horizon N_u are calculated in order to minimize some specified cost index J, possibly subject to constraints. The first control move of the sequence, $u(t/t)$, is applied to the real process, all the

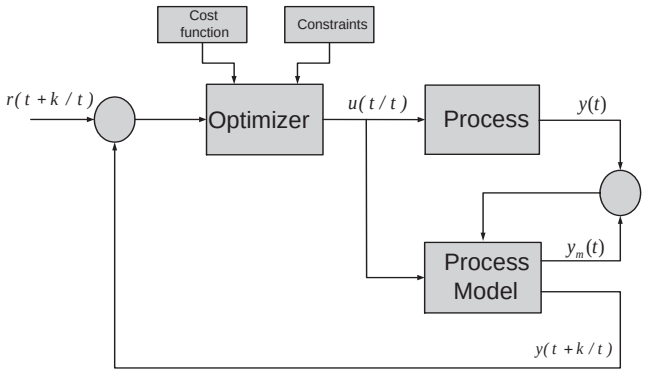

Figure 1: Block diagram of the MPC loop

other elements of the control vector are discarded and the calculations are repeated for the subsequent sampling instants. In order to account for the plant-model mismatch, a prediction error, $n(t)$, that is calculated based on plant measurement $y(t)$ and model output $y_m(t)$ is used to update the future predictions.

2.2 MIMO MPC

In this section, an extension of the MPC principles for MIMO systems is introduced. The exposition is restricted to the case of systems having two inputs and two outputs, since the application considered further falls into this category of systems, however the extension for systems with an arbitrary number of inputs and outputs is straightforward. General NMPC algorithms [16] have been developed, but they require the on-line solution of nonlinear optimization problems, which can be computationally demanding. Here the choice is made towards simplicity without sacrificing the performance. As particular approach to MPC the extended prediction self-adaptive control (EPSAC) algorithm [17] is used. The choice is therefore consistent in terms of an industrial application, with limited computer implementation.

The objective of a model predictive controller is to find the future process input sequence that optimizes a cost function over the prediction horizon N_p, taking the constraints on the process inputs and outputs into account. The simplest and most common cost index considers the summed squares of the predicted output deviations from the setpoint, although other terms such as penalties on the manipulated variables can also be included. For the clarity of the exposition, a two-input two-output system, for which u_i, y_i, r_i, $i = 1,2$ respectively denote the inputs, outputs and setpoints is used to present the concepts. However, these can be easily extended to systems having a higher number of inputs and outputs. Two alternatives may be considered:

1. only one optimization problem, which finds the two optimal control inputs that minimize one cost function (this case is referred to as solidary control):

$$\min_{\substack{u_1(t/t),\ldots,u_1(t+Nu-1/t)\\ u_2(t/t),\ldots,u_2(t+Nu-1/t)}} J \tag{1}$$

where

$$J=\sum_{k=1}^{N_p}[r_1(t+k|t)-y_1(t+k|t)]^2+[r_2(t+k|t)-y_2(t+k|t)]^2 \tag{2}$$

2. two optimization problems, each of them providing one optimal input minimizing one cost function (this case is referred to as selfish control):

$$\min_{u_1(t/t),\ldots,u_1(t+Nu-1/t)} J_1 \quad \text{and} \quad \min_{u_2(t/t),\ldots,u_2(t+Nu-1/t)} J_2 \tag{3}$$

where

$$J_1=\sum_{k=1}^{N_p}[r_1(t+k|t)-y_1(t+k|t)]^2 \tag{4}$$

$$J_2=\sum_{k=1}^{N_p}[r_2(t+k|t)-y_2(t+k|t)]^2 \tag{5}$$

Note that the selfish approach can be applied only for systems with an equal number of manipulated inputs and controlled outputs, while the solidary approach can be applied to any MIMO system.

The core of the EPSAC formulation for nonlinear systems is the replacement of the complex, time consuming nonlinear optimization with iterative quadratic optimization problems, whose solutions converge to the nonlinear optimal solution. To this end, the future sequence of manipulated variables $u_i(t+k|t)$, $i=1,2$, $k=0\ldots N_p-1$ (with $u_i(t+j/t)=u_i(t+N_u-1/t)$ for $j=N_u\ldots N_p-1$) is considered to be the sum of a basic future control scenario, $u_{i,base}(t+k|t)$, and optimizing future control actions $\delta u_i(t+k|t)$:

$$u_1(t+k|t)=u_{1,base}(t+k|t)+\delta u_1(t+k|t) \tag{6}$$

$$u_2(t+k|t)=u_{2,base}(t+k|t)+\delta u_2(t+k|t) \tag{7}$$

Consequently, the output predictions can be considered, in a first approximation, as being the cumulative result of two effects:

$$y_1(t+k|t)=y_{1,base}(t+k|t)+y_{1,opt}(t+k|t) \tag{8}$$

$$y_2(t+k|t)=y_{2,base}(t+k|t)+y_{2,opt}(t+k|t) \tag{9}$$

The components $y_{1,base}(t+k|t)$, $y_{2,base}(t+k|t)$, $k=1\ldots N_p$ are calculated applying the known (postulated) sequences $u_{1,base}(t+k|t)$, $u_{2,base}(t+k|t)$ to the nonlinear model inputs. The other components, $y_{1,opt}(t+k|t)$, $y_{2,opt}(t+k|t)$ are the responses to the optimizing components $\delta u_1(t+k|t)$, $\delta u_2(t+k|t)$. At this point, (8), (9) are only approximations based on the use of superposition principle.

Assuming the optimizing components of the control actions $\delta u_i(t+k|t)$ are small enough, it is possible to obtain an expression for $y_{i,opt}(t+k|t)$ by linearizing the model along the trajectories described by $u_{i,base}(t+k|t)$. Thus, $y_{i,opt}(t+k|t)$ are the cumulative effects of a series of impulse inputs and step inputs [17]:

$$\begin{aligned} y_{1,opt}(t+k|t) &= h_k^{11}\delta u_1(t|t) + h_{k-1}^{11}\delta u_1(t+1|t) + \ldots + \\ &+ g_{k-N_u+1}^{11}\delta u_1(t+N_u-1|t) + \\ &+ h_k^{12}\delta u_2(t|t) + h_{k-1}^{12}\delta u_2(t+1|t) + \ldots + \\ &+ g_{k-N_u+1}^{12}\delta u_2(t+N_u-1|t) \qquad (10) \\ y_{2,opt}(t+k|t) &= h_k^{21}\delta u_1(t|t) + h_{k-1}^{21}\delta u_1(t+1|t) + \ldots + \\ &+ g_{k-N_u+1}^{21}\delta u_1(t+N_u-1|t) + \\ &+ h_k^{22}\delta u_2(t|t) + h_{k-1}^{22}\delta u_2(t+1|t) + \ldots + \\ &+ g_{k-N_u+1}^{22}\delta u_2(t+N_u-1|t) \qquad (11) \end{aligned}$$

where the parameters h_k^{ij}, $k=1\ldots N_p$ are the coefficients of the local system unit impulse response, from input j to the output i, suitably calculated around the current operating trajectory by entering an impulse into the nonlinear model. The values g_k^{ij} refer to the unit step response coefficients, obtained similarly.

In matrix notations, the prediction equations are:

$$Y_1 = \bar{Y}_1 + G_{11}\cdot U_1 + G_{12}\cdot U_2 \qquad (12)$$

$$Y_2 = \bar{Y}_2 + G_{21}\cdot U_1 + G_{22}\cdot U_2 \qquad (13)$$

where

$$\begin{aligned} Y_i &= \left[\begin{array}{cccc} y_i(t+1|t) & \ldots & y_i(t+N_p|t) \end{array}\right]^T \\ \bar{Y}_i &= \left[\begin{array}{cccc} y_{i,base}(t+1|t) & \ldots & y_{i,base}(t+N_p|t) \end{array}\right]^T \\ U_i &= \left[\begin{array}{cccc} \delta u_i(t|t) & \ldots & \delta u_i(t+N_u-1|t) \end{array}\right]^T \qquad (14) \\ G_{ij} &= \left[\begin{array}{ccccc} h_1^{ij} & 0 & 0 & \ldots & 0 \\ h_2^{ij} & h_1^{ij} & 0 & \ldots & 0 \\ \vdots & \vdots & \vdots & \vdots & \vdots \\ h_{N_p}^{ij} & h_{N_p-1}^{ij} & h_{N_p-2}^{ij} & \ldots & g_{N_p-N_u+1}^{ij} \end{array}\right] \end{aligned}$$

Hence (2) may be rewritten as

$$J = ((R_1 - \bar{Y}_1) - G_1 \cdot U)^T \cdot ((R_1 - \bar{Y}_1) - G_1 \cdot U) + ((R_2 - \bar{Y}_2) - G_2 \cdot U)^T \cdot ((R_2 - \bar{Y}_2) - G_2 \cdot U) \quad (15)$$

with

$$G_1 = \begin{bmatrix} G_{11} & G_{12} \end{bmatrix} \quad G_2 = \begin{bmatrix} G_{21} & G_{22} \end{bmatrix} \quad U = \begin{bmatrix} U_1 \\ U_2 \end{bmatrix} \quad (16)$$

while (4) and (5) may be rewritten as

$$J_1 = (R_1 - \bar{Y}_1 - G_{11} \cdot U_1 - G_{12} \cdot U_2)^T \cdot (R_1 - \bar{Y}_1 - G_{11} \cdot U_1 - G_{12} \cdot U_2) \quad (17)$$

$$J_2 = (R_2 - \bar{Y}_2 - G_{22} \cdot U_2 - G_{21} \cdot U_1)^T \cdot (R_2 - \bar{Y}_2 - G_{22} \cdot U_2 - G_{21} \cdot U_1) \quad (18)$$

Thus the optimization problems (1) – the minimization of J – and (3) – the minimizations of J_1 and J_2 – possibly subject to constraints can be solved with standard quadratic programming (QP) techniques.

Notice that, as (8), (9) are only approximations, the control sequences $u_1(t+k|t) = u_{1,base}(t+k|t) + \delta u_1(t+k|t)$, $u_2(t+k|t) = u_{2,base}(t+k|t) + \delta u_2(t+k|t)$ are suboptimal. However, if the approach is repeated iteratively at the same sampling instant by redefining , $u_{1,base}(t+k|t) \equiv u_1(t+k|t)$, $u_{2,base}(t+k|t) \equiv u_2(t+k|t)$ and recalculating $\delta u_i(t+k|t)$ and $u_i(t+k|t)$ until $\delta u_i(t+k|t) \approx 0$, $i = 1,2$, i.e. $|\delta u_i(t+k|t)| \leq \varepsilon$, where ε is a small positive number, it converges to the optimal control sequence. In this way, the nonlinear optimization problem is replaced by several QP problems [17].

3 Process model

The animal cell culture used in this study is described by a model, which considers that the cells grow on glucose and glutamine and their death is governed by lactate, ammonia and glutamine concentrations. A schematic representation of the perfusion culture is given in Figure 2. Medium containing glucose and glutamine is continuously supplied to the reactor. Components leave the reactor at the same rate. The amount of cells in the effluent is determined by the filtration device.

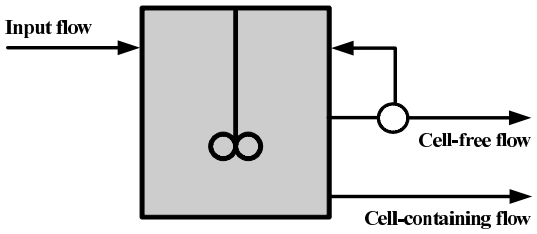

Figure 2: Schematic representation of the perfusion culture

The mathematical model of the system illustrated in Figure 2 is given by:

$$\dot{\xi}_1 = -bl \cdot D\xi_1 + r_1(\xi) - r_2(\xi) \tag{19}$$

$$\dot{\xi}_2 = D\xi_{in_2} - D\xi_2 - ar_1(\xi) - r_3(\xi) \tag{20}$$

$$\dot{\xi}_3 = D\xi_{in_3} - D\xi_3 - br_1(\xi) \tag{21}$$

$$\dot{\xi}_4 = -D\xi_4 + cr_1(\xi) + dr_3(\xi) \tag{22}$$

$$\dot{\xi}_5 = -D\xi_5 + er_1(\xi) \tag{23}$$

where

- ξ_1, ξ_2, ξ_3, ξ_4, ξ_5 respectively represent the concentrations of viable cells, glucose, glutamine, lactate and ammonia.
- $D = F/V$ is the dilution rate and $bl \in [0,1]$ is the bleed ratio
- $r_i(\xi)$, $i = 1,2,3$ are reaction rates, given by:

$$\begin{aligned} r_1(\xi) &= \mu_{max} \cdot \frac{\xi_2}{K_{Glc} + \xi_2} \cdot \frac{\xi_3}{K_{Gln} + \xi_3} \cdot \xi_1 \\ &= \mu_1(\xi) \cdot \xi_1 \end{aligned} \tag{24}$$

$$\begin{aligned} r_2(\xi) &= \frac{k_{d_{max}}}{\mu_{max} - k_{d_{Lac}}\xi_4} \cdot \frac{1}{\mu_{max} - k_{d_{Amm}}\xi_5} \cdot \frac{k_{d_{Gln}}}{k_{d_{Gln}} + \xi_3} \cdot \xi_1 \\ &= \mu_2(\xi) \cdot \xi_1 \end{aligned} \tag{25}$$

$$\begin{aligned} r_3(\xi) &= m_{Glc} \cdot \frac{\xi_2}{k_{m_{Glc}} + \xi_2} \cdot \xi_1 \\ &= \mu_3(\xi) \cdot \xi_1 \end{aligned} \tag{26}$$

$\mu_1(\xi)$ is the growth function, which expresses that cell growth is limited by the availability of the two substrates (glucose and glutamine). $\mu_2(\xi)$ is the death function, which indicates that cell death is enhanced by the accumulation of inhibiting metabolites (ammonia, lactate) and the depletion

of the fundamental substrate glutamine. A part of the substrate glucose is not used for cell growth purposes but for cell maintenance activities as expressed by $\mu_3(\xi)$.

- $a, b, c, d, e > 0$ are the stoichiometric coefficients, defined as: $a = \frac{1}{Y_{X_v/Glc}}$, $b = \frac{1}{Y_{X_v/Gln}}$, $c = \frac{Y_{Lac/Glc}}{Y_{X_v/Glc}}$, $d = Y_{Lac/Glc}$, $e = \frac{Y_{Amm/Gln}}{Y_{X_v/Gln}}$.

  Product formation (lactate, ammonia) accompanies substrates consumption through the stoichiometric coefficients that express a related yield.

The model (19)-(23) does not include the dynamics of the dead cells concentration as this variable does not influence any of the system states. Including dead cells concentration as a system state would be interesting for determining the culture viability (given by the ratio between the viable cells and the sum of viable and dead cells), however such a variable cannot be easily measured (the only possible way is the count under the microscope of the cells).

This model has been developed from batch and fed-batch hybridoma culture results [18]. The model parameters are given in Table 1. It is expected that the model is valid also in the case of operating the system in perfusion mode, as the kinetic parameters are always identified from batch and fed-batch experiments. Compared to the fed-batch mode, a perfusion culture will reach higher cell concentration at steady state, however the main advantage is its continuous operation (long-term operation). This results in the use of smaller bioreactors, the continuous purification of the produced biomolecule and less downtime of the system.

Table 1: Numerical values of the animal cell culture (as in [18])

$Y_{X_v/Glc}$	$1.09 \cdot 10^2$	10^6 cells/mmol
$Y_{X_v/Gln}$	$3.8 \cdot 10^2$	10^6 cells/mmol
$Y_{Lac/Glc}$	1.8	mmol/mmol
$Y_{Amm/Gln}$	0.85	mmol/mmol
μ_{max}	1.09	day^{-1}
$k_{d_{max}}$	0.69	day^{-1}
V	0.8	L
K_{Glc}	1	mmol/L
K_{Gln}	0.3	mmol/L
$k_{d_{Lac}}$	0.01	day^{-1}(mmol/L)$^{-1}$
$k_{d_{Amm}}$	0.06	day^{-1}(mmol/L)$^{-1}$
$k_{d_{Gln}}$	0.02	mmol/L
m_{Glc}	$1.68 \cdot 10^{-4}$	mmol(10^6 cells)$^{-1}$day^{-1}
$k_{m_{Glc}}$	19	mmol

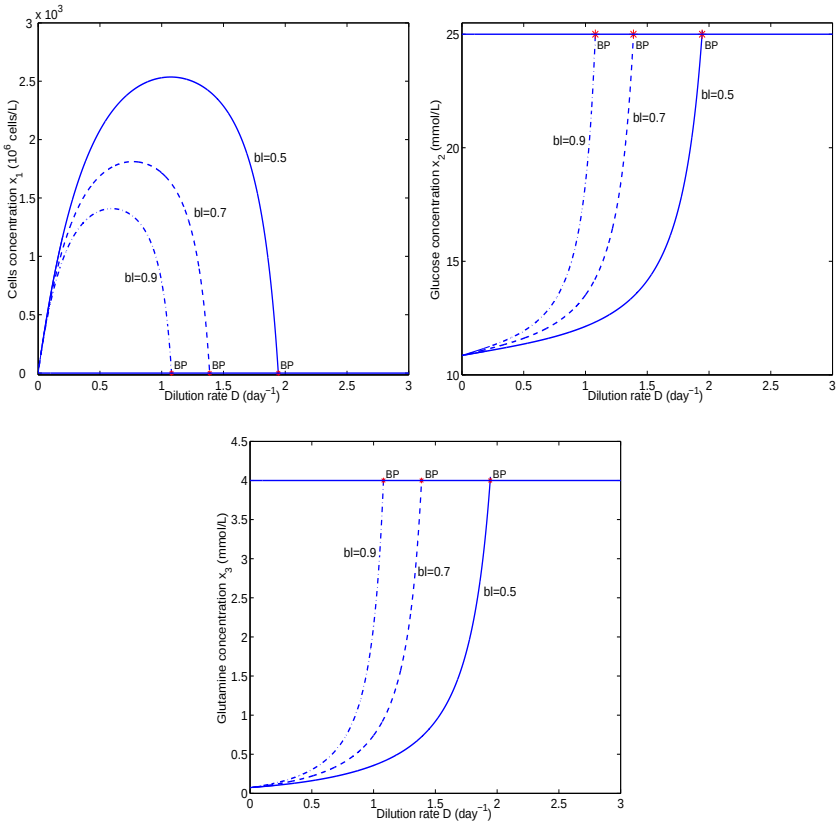

Figure 3: Bifurcation diagrams of the canonical model

3.1 Steady state analysis

A good knowledge of the system behaviour is necessary to develop an efficient and robust control strategy. In this section, the steady state behaviour of the animal cell culture (19)- (23) is analyzed. To ease the analysis, a well known transformation for biochemical systems to a canonical form is used [19]. By considering the partition and the transformation of the states as

$$x_a = \begin{bmatrix} x_1 \\ x_2 \\ x_3 \end{bmatrix} = \begin{bmatrix} \xi_1 \\ \xi_2 \\ \xi_3 \end{bmatrix} \tag{27}$$

$$x_b = \begin{bmatrix} x_4 \\ x_5 \end{bmatrix} = \begin{bmatrix} \xi_4 \\ \xi_5 \end{bmatrix} - C_b C_a^{-1} \begin{bmatrix} \xi_1 \\ \xi_2 \\ \xi_3 \end{bmatrix} \tag{28}$$

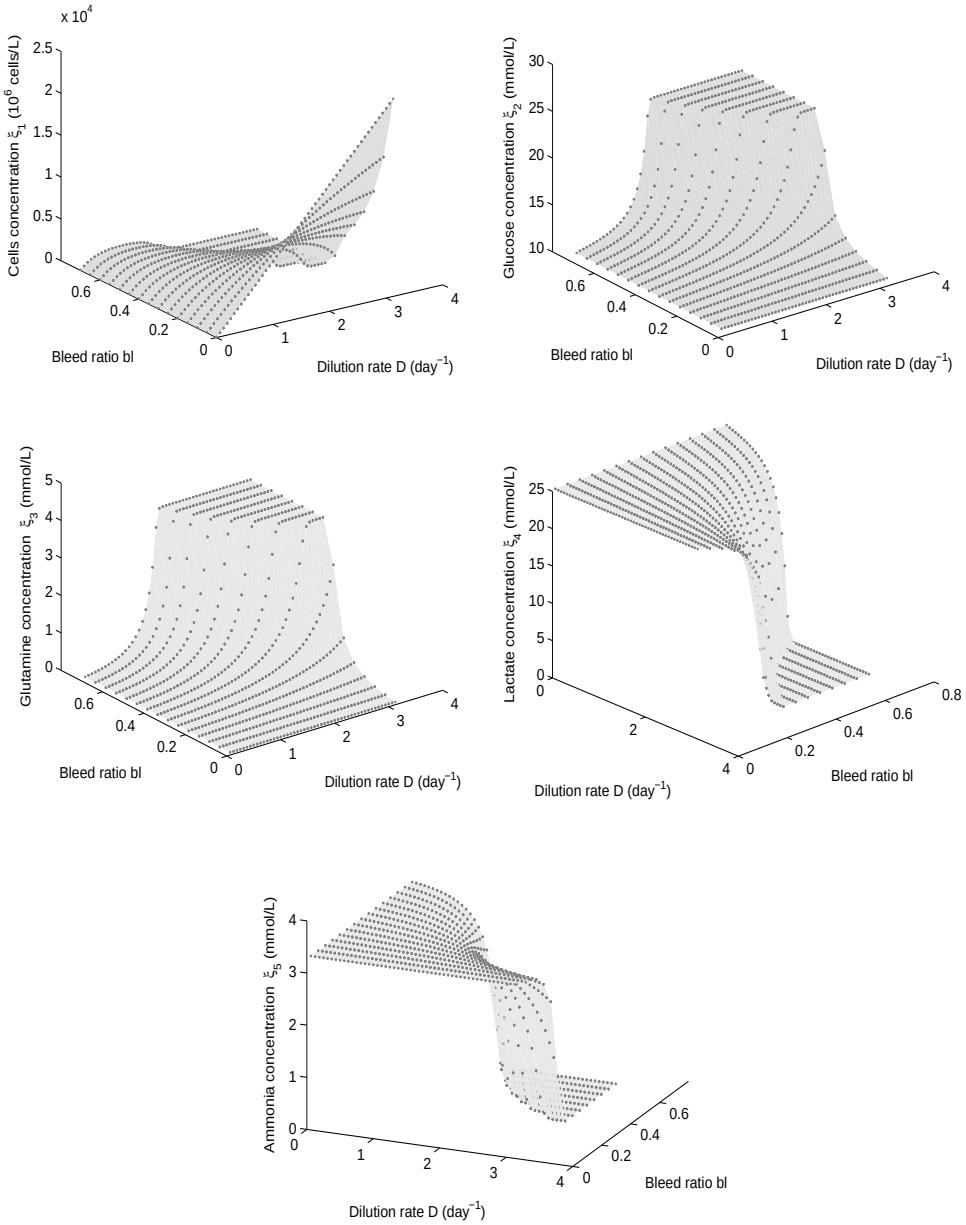

Figure 4: The steady states of the animal cell culture

where

$$C_a = \begin{bmatrix} 1 & -1 & 0 \\ -a & 0 & -1 \\ -b & 0 & 0 \end{bmatrix} \qquad C_b = \begin{bmatrix} c & 0 & d \\ e & 0 & 0 \end{bmatrix} \tag{29}$$

the canonical model of the system (19)-(23) is:

$$\dot{x}_1 = -bl \cdot Dx_1 + r_1(x) - r_2(x) \tag{30}$$
$$\dot{x}_2 = D(\xi_{in_2} - x_2) - ar_1(x) - r_3(x) \tag{31}$$
$$\dot{x}_3 = D(\xi_{in_3} - x_3) - br_1(x) \tag{32}$$
$$\dot{x}_4 = D(d\xi_{in_2} - x_4) \tag{33}$$
$$\dot{x}_5 = D(e/b\xi_{in_3} - x_5) \tag{34}$$

This model consists of a nonlinear part of dimension 3 dynamically coupled with a linear part of dimension 2. Its state space is

$$S_x = \Big\{ x \in \mathbb{R}^5; \xi_1 = x_1 \geq 0, \xi_2 = x_2 \geq 0, \xi_3 = x_3 \geq 0, \\ \xi_4 = x_4 - dx_2 \geq 0, \xi_5 = x_5 - e/bx_3 \geq 0 \} \tag{35}$$

and, as time increases, its dynamics converge to the space

$$\Delta = \{x_1 \geq 0, x_2 \geq 0, x_3 \geq 0, x_4 = d\xi_{in_2}, x_5 = e/b\xi_{in_3}\} \tag{36}$$

The steady states of the canonical model can be computed by setting the derivatives in (30)-(34) equal to zero. Besides the wash out solution

$$x^w = \begin{bmatrix} 0 & \xi_{in_2} & \xi_{in_3} & d\xi_{in_2} & e/b\xi_{in_3} \end{bmatrix}^T,$$

which occurs independently of the values of perfusion and bleed rates, the system may possess one or more non-trivial steady states, given by:

$$\mu_1(x) - \mu_2(x) - bl \cdot D = 0 \tag{37}$$
$$D(\xi_{in_2} - x_2) - (a\mu_1(x) + \mu_3(x))x_1 = 0 \tag{38}$$
$$D(\xi_{in_3} - x_3) - b\mu_1(x)x_1 = 0 \tag{39}$$
$$x_4 = d\xi_{in_2} \tag{40}$$
$$x_5 = e/b\xi_{in_3} \tag{41}$$

Due to the complexity of the kinetics, it will not generally be possible to derive analytical expressions of the steady states, however useful relationships and conditions between the system states and the inputs may be found. For example,

denoting by x^* a non-trivial steady state of (30)-(34) (i.e. the states of x^* are solutions of (37)-(41)), (38) and (39) result in

$$x_1^* = \frac{D(\xi_{in_2} - x_2^*)}{(a\mu_1(x^*) + \mu_3(x^*))} \tag{42}$$

$$x_1^* = \frac{D(\xi_{in_3} - x_3^*)}{b\mu_1(x^*)} \tag{43}$$

Since x_1^* represents the concentration of cells at equilibrium, the right hand sides of (42) and (43) must be positive, which imply that:

$$x_2^* \leq \xi_{in_2} \tag{44}$$

$$x_3^* \leq \xi_{in_3} \tag{45}$$

Further, eliminating x_1^* from (42) and (43) leads to

$$\frac{(\xi_{in_3} - x_3^*)}{(\xi_{in_2} - x_2^*)} = \frac{a}{b} + \frac{\mu_3(x^*)}{b\mu_1(x^*)} \tag{46}$$

which expresses the relationship between the concentration of the two nutrients at equilibrium.

The steady state multiplicity character of a system is an important aspect in the development and performance evaluation of a control strategy. Therefore, knowing the number and stability properties of the non-trivial solutions could be useful in the process of designing and tuning the controller. A priori, one does not expect the occurrence of multiple non-trivial steady states of the system (30)-(34), as substrate limitation has proven not to be one of the mechanisms triggering this phenomenon in biological systems with constant yield coefficients [20]. Nevertheless, this may be checked by numerically constructing the bifurcation diagrams of system (30)-(34) using interactive continuation tools [21]. The bifurcation diagrams are shown in Figure 3.

The bifurcation diagrams represented in Figure 3 are graphical illustrations of the steady state values of the nonlinear states x_1, x_2, x_3 (respectively cell, glucose and glutamine concentrations) as functions of the dilution rate, while a constant value of the bleed ratio has been assumed. The diagrams have been generated for three distinct values of the bleed ratio, namely 0.5, 0.7 and 0.9. For each of these bleed ratios, the diagram consists of two branches: i) one horizontal line ($x_1 = 0$, $x_2 = \xi_{in_2}$, $x_3 = \xi_{in_3}$), which corresponds to the wash out steady state x^w; and ii) a second branch along which x_1, x_2, x_3 assume different values depending on the dilution rate, which corresponds to the non-trivial steady state x^*. Thus, only one non-trivial solution may occur. For a certain value of the dilution rate D^{BP}, the two branches intersect in the branch point (BP), the one corresponding

to the non-trivial solution leaving the physical state space (this means that conditions (44), (45) are not fulfilled). Thus, for dilution rates higher than the the corresponding D^{BP} for a given bleed ratio, the only physical steady state is the wash out, which is globally asymptotically stable in this case. For dilution rates smaller than the corresponding D^{BP}, the non-trivial solution is asymptotically stable, while the wash out is unstable. Noticeable is the fact that, as the bleed ratio increases, the branch point moves to lower dilution rate, thus decreasing the range of dilutions for which a non-trivial physical steady state exists. This may also be noticed in Figure 4, which presents the static characteristic (reachable steady states) of the animal cell culture for various combinations of dilution rate and bleed ratio.

4 Simulation results and discussion

One of the main objectives in animal cell cultures is to achieve and maintain a high cell density in the reactor. As the dynamics of such systems converge to a steady state, a proper scaling of the process and appropriate selection of the perfusion and bleed rates could lead in principle to the desired cells concentration, however the growth may take a considerable amount of time, the process may be affected by disturbances (variation of the kinetic parameters, perturbations related to maintenance interventions such as changing gas reservoirs or medium collecting bottles, harvesting, etc) or large amounts of expensive nutrients may leave the reactor. For these reasons a control strategy is usually used to achieve the goal and correct undesired influences on the process.

Since the bleed rate has been rarely used in a control loop (usually it was manually set to specific values for reaching a constant cell concentration [22]), the most encountered control strategies for animal cell cultures either regulate the concentration of toxic byproducts (such as lactate) or the concentration of a nutrient (mostly glucose) by manipulating the perfusion rate. As only one input may be manipulated, but there are many factors influencing the cell growth, the possibilities of optimizing such processes are quite limited. In any case, finding good optimization criteria, which take into account the biological complexity but also economical aspects, is difficult. Nevertheless, adding another degree of freedom, by using the bleed rate as manipulated variable in a control loop offers more opportunities for process optimization and tighter control.

In this section, simulation results regarding the control of the animal cell culture (19)-(23) using the MIMO predictive strategy introduced in section 2 are presented. The manipulated variables are the dilution rate D and the bleed ratio bl, while the controlled variables are the cell concentration ξ_1 and glucose concentration ξ_2. Both solidary and selfish approaches are investigated. The manipulated

variables are constrained as follows:

$$0 \leq bl \leq 1 \tag{47}$$

$$0 \leq D \leq 3.75\text{day}^{-1} \tag{48}$$

While the motivation of controlling the cell concentration is evident, the choice of regulating the glucose concentration might not be so straightforward. Aside the fact that the optimal operation of the animal cell culture is a function of the extent of medium utilization (defined as the difference between the nutrients concentration in the influent and in the effluent) [22], many studies (see [5] and the references therein) have revealed that low levels of glucose and glutamine in the medium lead to a better usage of these nutrients in an energy efficient manner. Moreover, the medium is the most costly element in cell cultures and it will be continuously refreshed in the perfusion systems. Thus, the objective of the control loop is to move the system from one steady state to another one, possibly characterized by a higher concentration of cells and a lower concentration of glucose. As these type of systems converge to a steady state, the states corresponding to high cell concentration can be computed using the model, hence no optimization procedure to determine the maximum amount of cells is needed.

4.1 Transient start-up

Figure 5 illustrates the system open loop response versus the controlled response. The open loop response shown with continuous line is obtained by setting constant perfusion and bleed rates. These correspond to the steady states characterized by the cell and glucose concentrations represented with horizontal lines and chosen as the setpoints for the control loop. These particular steady states serve as a first example for our goal of controlling the animal cell culture at higher cell concentration and lower glucose concentration. The second simulation, illustrated with dashed line, represents the system controlled response, when the selfish MIMO predictive controller is introduced in the loop. The controller parameters for both inputs and outputs are $N_u = 1$, $N_p = 5$. The sampling period is $T_s = 0.1$ day and this value will be further used in all simulation results. The other two simulation results represent the system responses controlled with a solidary MIMO predictive controller. The dash-dotted line shows the results when the controller parameters are set to $N_u = 1$, $N_p = 5$, while the dotted line is the response in the case $N_u = 1$, $N_p = 10$.

Figure 5 shows that a fast convergence to the setpoint is achieved, of both cell and glucose concentrations, the speed of the loop being increased several times compared to the open loop. In the case of the selfish approach, the dilution rate and bleed ratio are calculated to minimize both cost functions (4), (5), taking the full

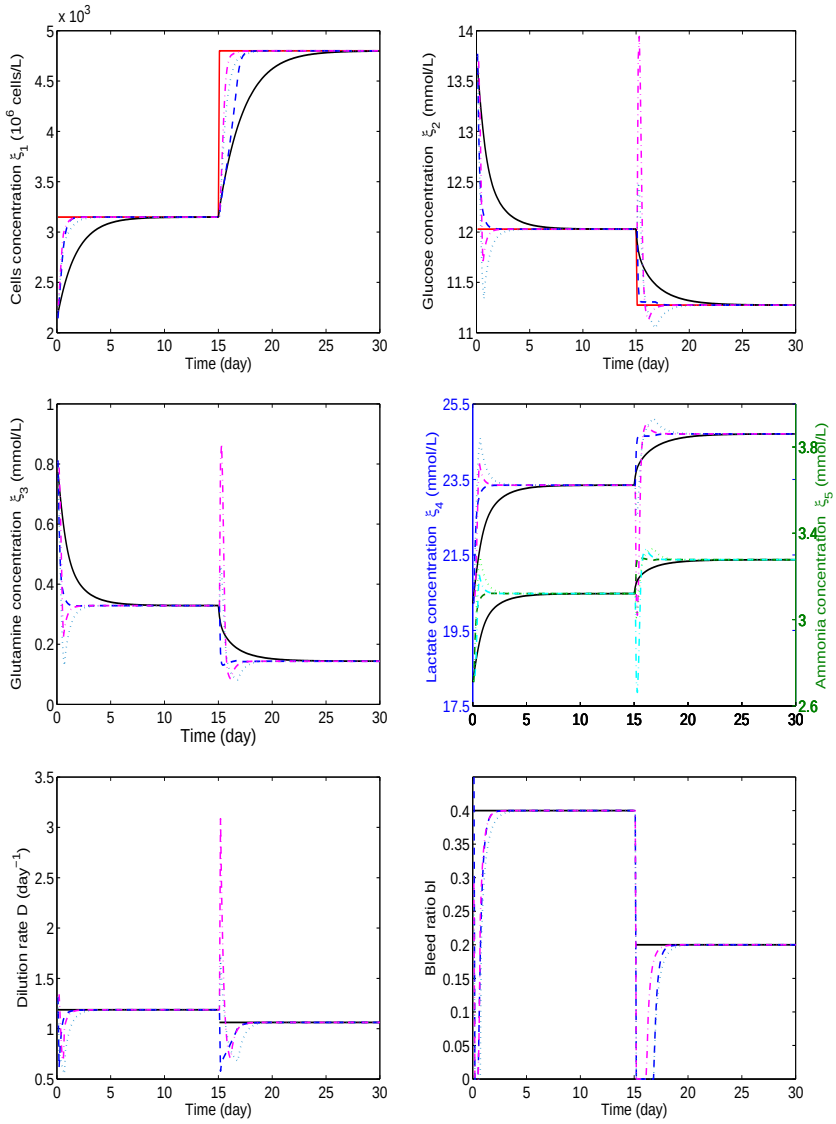

Figure 5: Open loop response (continuous line) and MIMO predictive control of cell and glucose concentrations for stepwise setpoint changes: selfish approach with $N_u = 1$, $N_p = 5$ - dashed line, solidary approach with $N_u = 1$, $N_p = 5$ - dash-dotted line, solidary approach with $N_u = 1$, $N_p = 10$ - dotted line. System initial state $\xi(0) = [2.21423e3 \quad 13.75 \quad 0.81 \quad 20.25 \quad 2.71]^T$

system dynamics (influence of each input on both outputs) into account. Although the formulation of selfish control might suggest a decoupled control (as the bleed ratio is manipulated to control the cell concentration and the perfusion rate is manipulated to control the glucose concentration), this is certainly not the case: the predictions of each of the two outputs are computed based on both postulated input sequences. This insures the internal cross compensation of the dynamic interactions rather than their rejection.

In the case of the solidary approach, the dilution rate and the bleed ratio are calculated to minimize the cost function (2), which states that the total control error in the system is minimized. This implies that it is possible to increase deliberately the control error on one of the controlled variable for reducing the control error on the other variable. This is obvious in Figure 5, where the glucose concentration increases at each setpoint change before decreasing to the desired value. This increase may be attenuated by using a larger prediction horizon.

In spite of the promising results displayed in Figure 5, there are situations when the selfish control strategy does not lead to a faster growth of the cells, although fulfilling the control objective. Such a situation is presented in Figure 6, which compares the system open loop response with the controlled responses. In the case of the selfish approach, the nutrients are rather transformed to metabolites than used for growth, the high concentration of lactate and ammonia promoting cell death. This is noticeable in the beginning of the simulation, when the cell concentration drops below the initial value. Further on, the cell concentration starts increasing, but the growth is limited by the low concentration of glucose and glutamine. Changing the controller parameters does not lead to an obvious improvement in the performance (Figure 7). Concluding, fast regulation of glucose to lower levels is not the most desirable control criterion (at least not for the selfish approach), especially in cases like this, when a high concentration of lactate is initially present in the reactor (approximately 24 mmol/L or above).

To overcome the problem of increased death rate and slow growth in the selfish approach, a change in the layout of the setpoint imposed for glucose concentration is considered. Instead of the step-wise setpoint change, a profile composed of a ramp followed by a constant level is chosen. Figure 8 shows the controlled response for two different values of the ramp slope. In the first case, a progressive decrease over a period of three days is imposed to the glucose concentration. Although a smooth increase in the cell concentration can be noted, the net growth rate is still small at the end of this phase, causing a sluggish system response. Nevertheless, compared to the open loop response, the controlled process reaches the desired cell concentration faster, the benefit in time being of approximately five days (from 14 days in open loop to 9 days in the controlled case). An even faster growth is achieved when the setpoint imposed to the glucose concentration decreases progressively during the first six days. In this case, the cell concentration

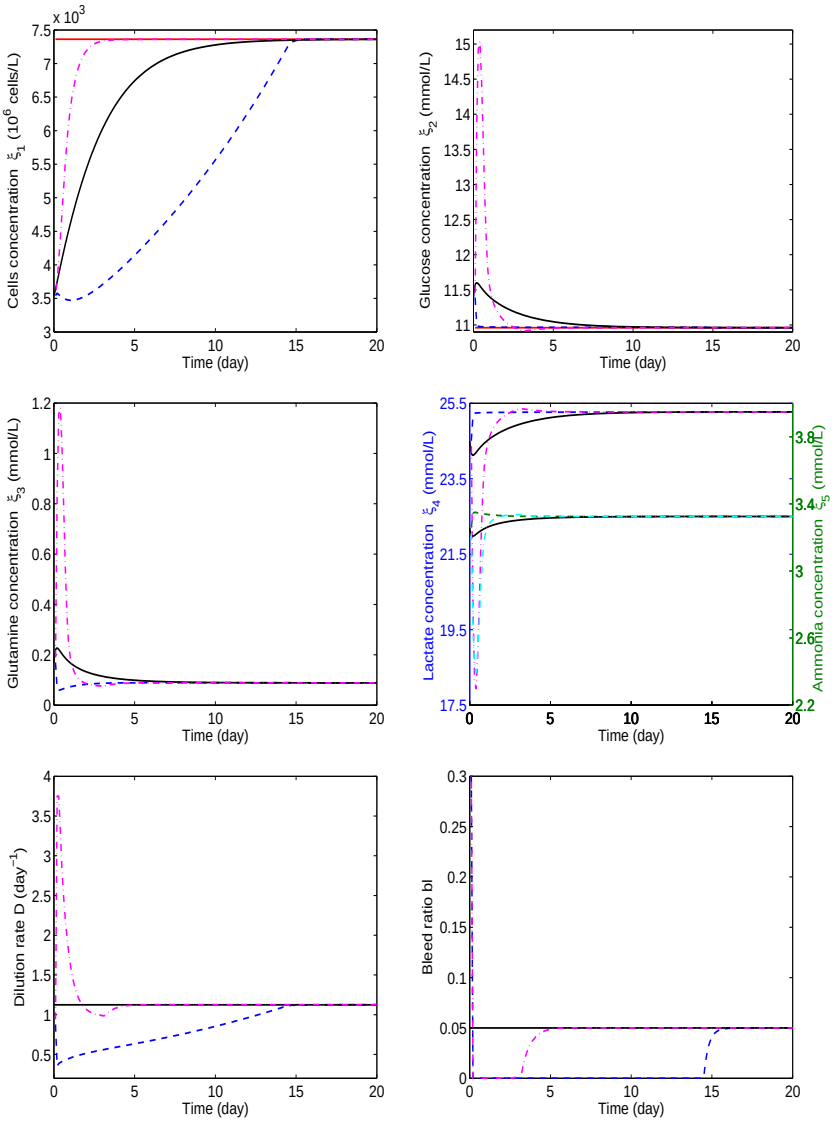

Figure 6: Open loop response (continuous line) and MIMO predictive control of cell and glucose concentrations for another setpoint: selfish approach with $N_u = 1$, $N_p = 5$ - dashed line, solidary approach with $N_u = 1$, $N_p = 10$ - dash-dotted line. System initial state $\xi(0) = [3.54292e3 \quad 11.39 \quad 0.17 \quad 24.51 \quad 3.26]^T$

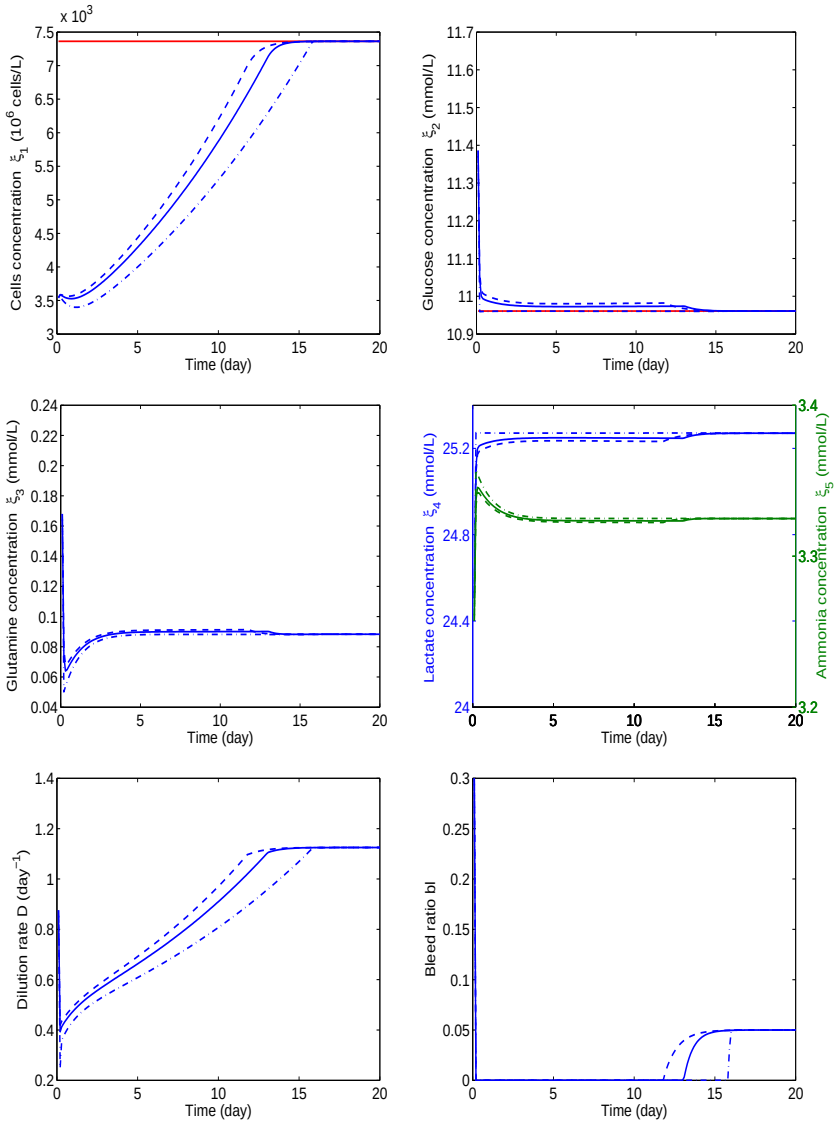

Figure 7: Selfish MIMO predictive control of cell and glucose concentrations: $N_u = 1$, $N_p = 10$ - continuous line, $N_u = 1$, $N_p = 15$ - dashed line, $N_u = 3$, $N_p = 10$ - dash-dotted line

reaches the desired level after only 4 days.

It is obvious that incorporating knowledge about the system dynamics in the control problem leads to a more effective solution. The progressive decrease of the glucose concentration used in the previous simulations has a great impact on how fast cells grow, however the way it has been introduced does not allow for formalization. This means that the slope of the ramp, which certainly influences the results, depends on the initial conditions as well as the desired values. Thus, it is not possible that a certain value of this parameter is well suited for all possible initial conditions and all possible desired values. Moreover, finding one or more values of this parameter implies extensive simulations of the control loop. Opposite to this approach, we relate these observations to some invariant property of the system (19)-(23), which provides a consistent manner for deriving the solution.

Figure 9 presents glucose concentration versus glutamine concentration for several situations: the dotted line represents the glucose and glutamine concentrations in steady state, calculated using the relationship (46) (this curve will be further referred to as the steady state curve); the continuous line is the representation of nutrients from the simulation illustrated in Figure 6, when the settling time for the cell concentration is approximately 15 days; the dashed and dash-dotted lines are respectively the representations of nutrients from the simulations illustrated in Figure 8, when the settling times for the cell concentration are 9 days and 4 days, respectively. According to these results, as closer the evolution of the nutrients to the steady state curve, as smaller the time needed by the cell to reach the desired concentration. Consequently, the control objective has been modified to accommodate this observation, namely a second term has been included in the cost index (5), which now becomes

$$J_2 = \sum_{k=1}^{N_p} [r_2(t+k|t) - \xi_2(t+k|t)]^2 + \\ + \alpha \sum_{k=1}^{N_p} [r_3(t+k|t) - \xi_3(t+k|t)]^2 \tag{49}$$

where α is a weighting coefficient, $\xi_3(t+k/t)$ are predictions of the glutamine concentration and $r_3(t+k/t)$ are predictions of the setpoint for the glutamine concentration. The setpoint for the glutamine concentration $r_3(t)$ is the steady state glutamine concentration x_3^* corresponding to the current value of the glucose concentration $\xi_2(t)$ and is found from (46), where $x_2^* = \xi_2(t)$. The weighting coefficient α was set to the value 100 in the subsequent simulations, to account for the difference in the magnitude of glucose and glutamine concentrations.

Figure 10 shows the system controlled response when the cost index (49) is used for optimization. The same setpoint change in the cell concentration as in

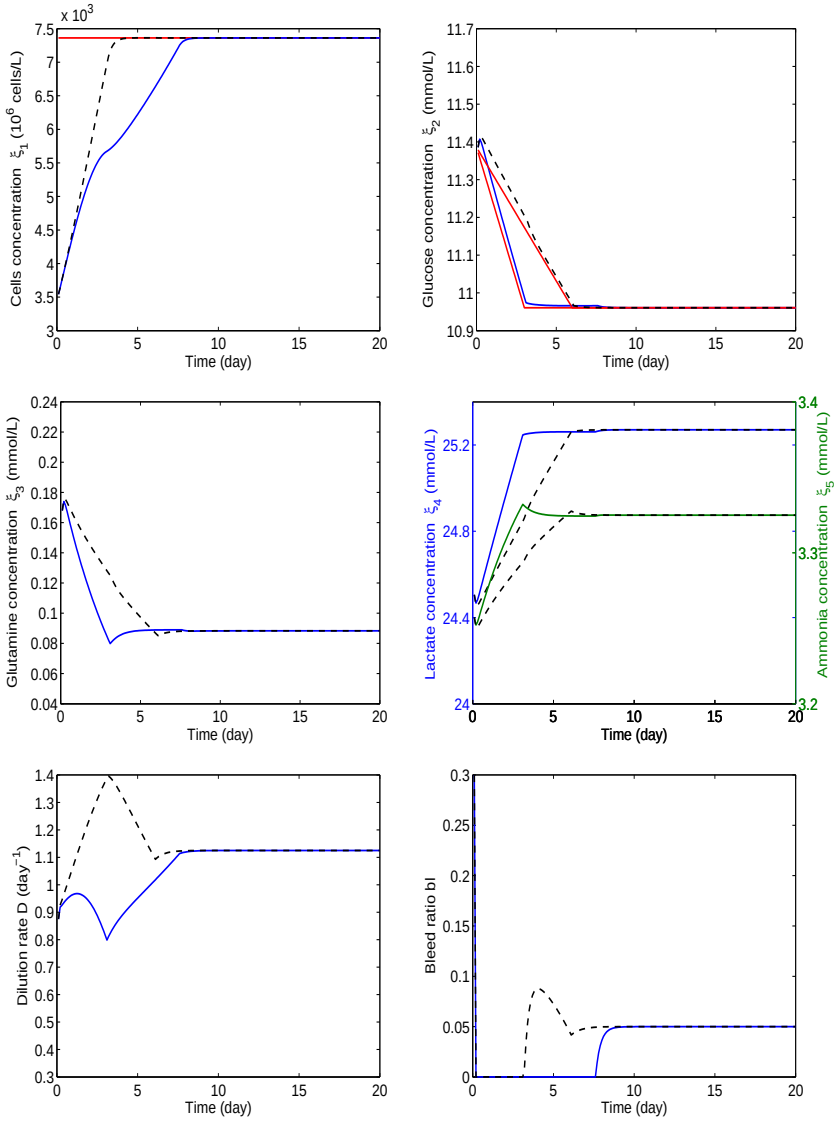

Figure 8: Controlled system response for ramp-like setpoints for the glucose concentration: selfish approach with $N_u = 1$, $N_p = 5$

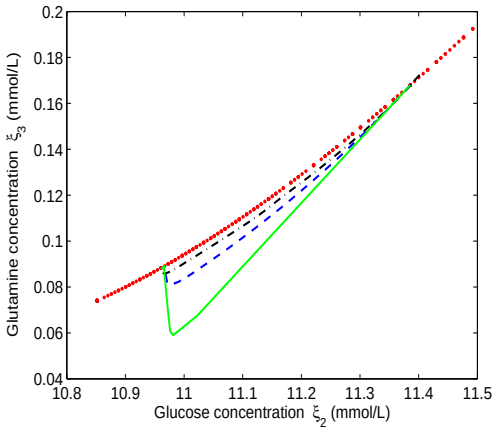

Figure 9: Glutamine concentration versus glucose concentration: steady state (dotted line), controlled case shown in Figure 6 (continuous line), controlled cases shown in Figure 8 (dashed and dash-dotted lines)

Figures 6, 8 is used and the settling time for the cell concentration is comparable (approximatively 4.5 days) to the one obtained by imposing the six days ramp-like decrease on the glucose concentration or the one obtained with the solidary approach. The new formulation allows for a successful control result for other initial and final conditions, without additional investigations. Figure 11 illustrates the effectiveness of the proposed strategy for a more significant setpoint change on the cell concentration, situation where also limitations on the perfusion rate occur. The controlled system response with the solidary approach is also shown. In this case, the prediction horizon has been increased to $N_p = 15$ to insure the closed loop stability.

4.2 Disturbance rejection

Figure 12 shows the case when the reactor is disturbed by replacing part of its volume with fresh medium. In the first case 25% of the reactor volume is replaced, in the second case 50% of the reactor volume is replaced. The controller, implemented either in the selfish approach or in the solidary approach, successfully brings back the system to the desired setpoint, the cell concentration reaching the setpoint in a short period of time.

4.3 Solidary versus selfish control

The simulation results show that both approaches are able to drive the system to the imposed setpoints, however there are some differences which should be

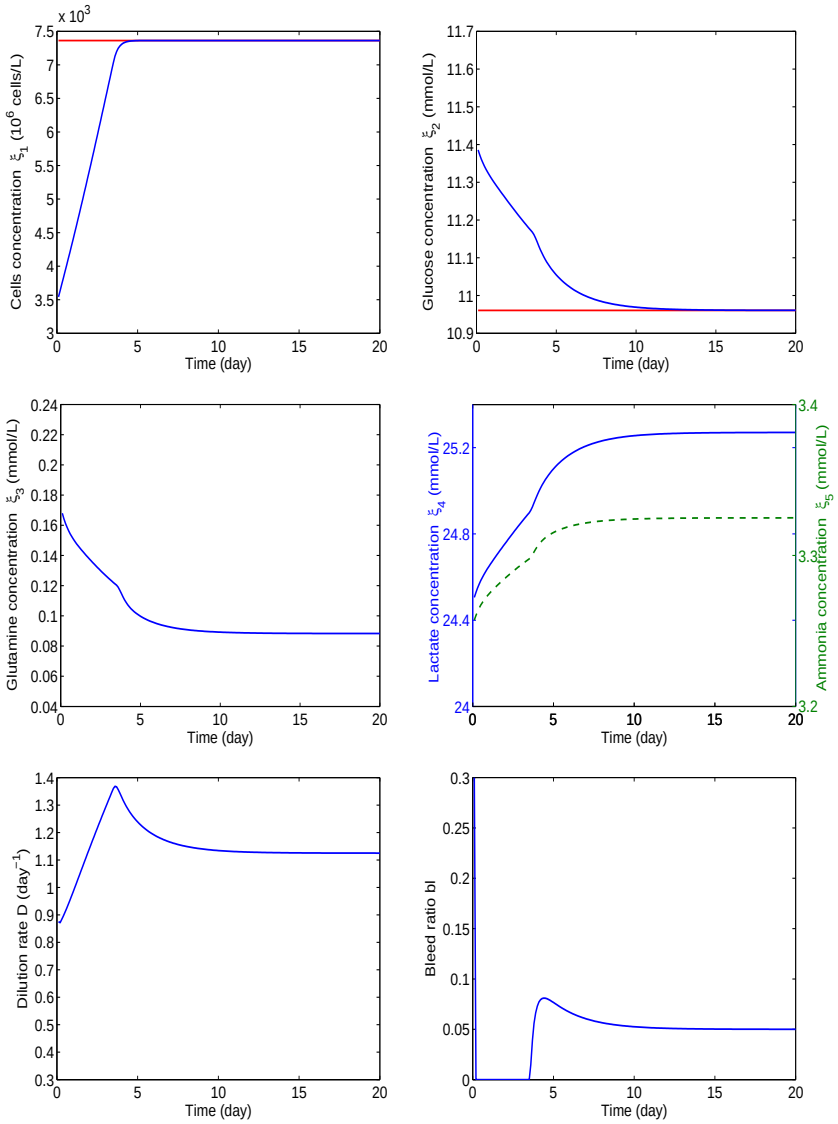

Figure 10: Selfish MIMO predictive control of cell and glucose concentrations: modified cost index

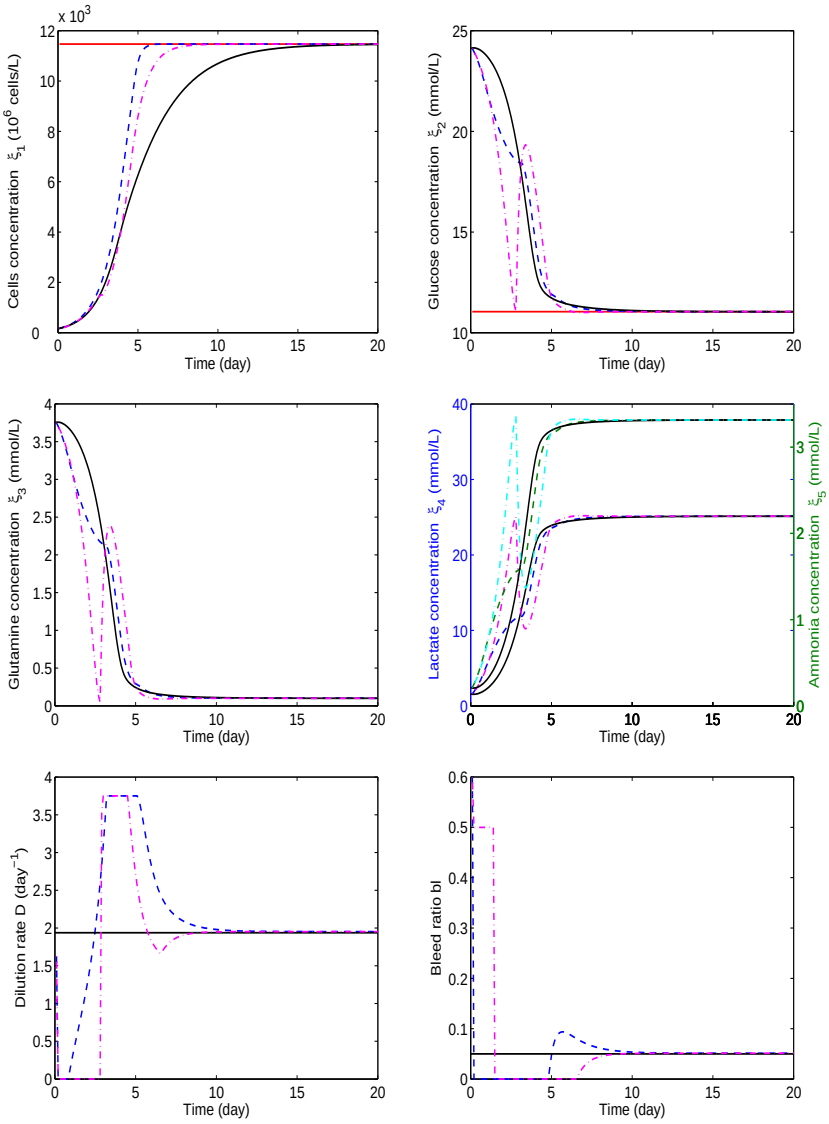

Figure 11: Open loop response (continuous line) and MIMO predictive control of cell and glucose concentrations for higher cell concentration setpoint: selfish approach with modified cost index, $N_u = 1$, $N_p = 5$ - dashed line, solidary approach with $N_u = 1$, $N_p = 15$ - dash-dotted line. System initial state $\xi(0) = [1.57698e2 \quad 24.12 \quad 3.75 \quad 1.58 \quad 0.21]^T$

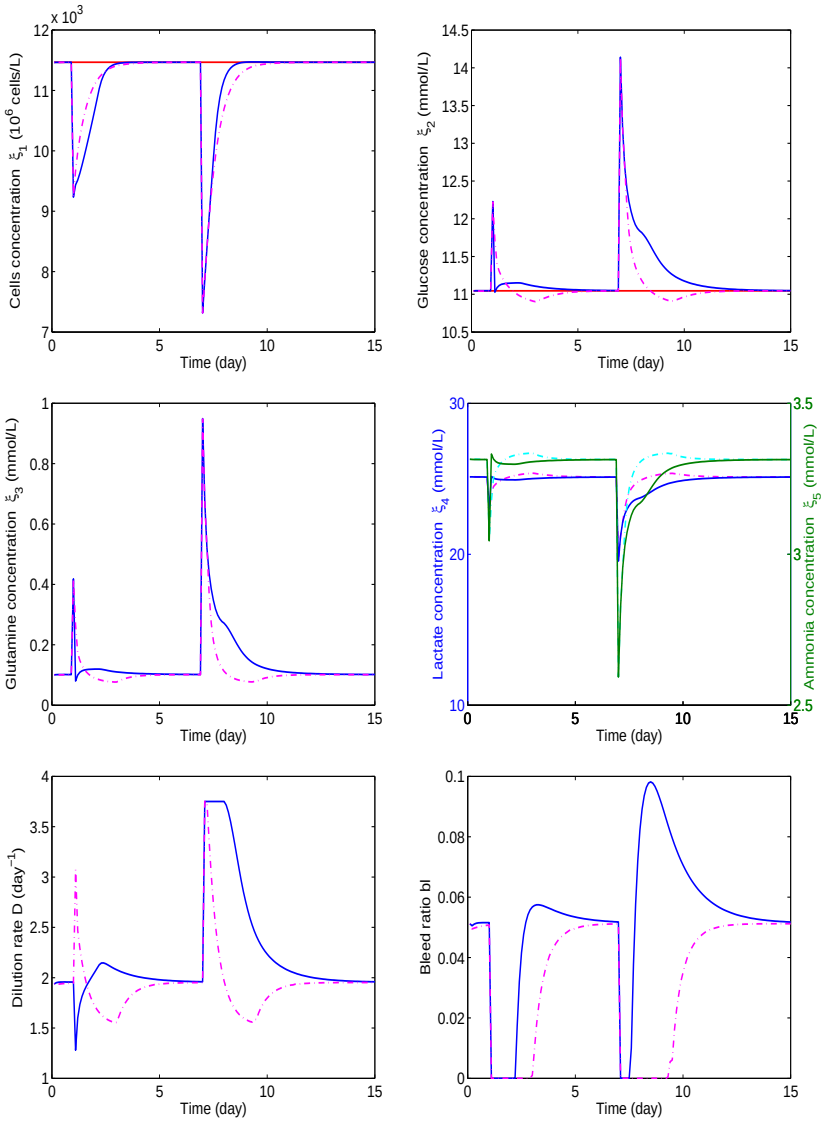

Figure 12: Disturbance rejection: selfish approach with modified cost index, $N_u = 1$, $N_p = 5$ - continuous line, solidary approach with $N_u = 1$, $N_p = 10$ - dash-dotted line

taken into account when selecting one approach or the other. The solidary control results in a fast regulation of the outputs to the imposed setpoints, with almost identical settling time for both outputs. However, a large increase in the glucose concentration occurs at each setpoint change to boost up the growth of the cells. Additionally, reasonably large prediction horizons must be used, especially when a significant change on the cell concentration setpoint is imposed, in order to insure the closed loop stability. On the other hand, the selfish approach is able to preserve stability even for small prediction horizons, but an imbalance in the speed of the two loops will occur when imposing setpoints with higher cell concentration and lower glucose concentration, the regulation of the glucose being much faster than the regulation of the cell concentration. The cells growth can be speed up in the selfish approach by considering the modified cost index. In this case, a continuous decrease in the glucose concentration is achieved. Using higher values for the control horizon was not necessary as reasonably good results were obtained for $N_u = 1$. Regarding the number of the QP problems solved at each sampling instant, the solidary approach needed at most four iterations during the transient period of the simulation shown in Figure 6, while the solidary approach with the modified cost index needed at most three iterations during the transient period of the simulation illustrated in Figure 10. The stop condition for the iterative computation of the optimal input is $|\delta u_i(t+k/t)| \leq 1e-5$.

5 Conclusions

In this paper multivariable predictive control has been used efficiently to simultaneously control cell and glucose concentrations in an animal cell culture operated in perfusion mode. The controller calculates the optimal dilution and bleed rates to drive the system to the desired steady state. Two approaches have been considered: the solidary approach which computes the optimal controls by minimizing the total control error in the system and the selfish approach which computes the optimal controls by minimizing the control error on each output. Although faster regulation of both outputs is achieved occasionally with the solidary approach, the simulation results presented here indicate the selfish approach with the modified cost index a better alternative for the real-life implementation. Aside the low computational effort required by this particular MPC algorithm, i) no stability issues related to the choice of the prediction horizon were encountered in the selfish approach, ii) a continuous decrease of the glucose concentration was achieved, iii) less control effort was needed to achieve the goal.

Control of animal cell cultures by manipulating both flows is largely unexplored. On top of that, multivariable control raises always interesting problems, due to process interactions, especially in biological systems. Thus, this paper

points out to some interesting features of animal cell cultures, providing at the same time an efficient solution. Further research work is currently devoted to the exploration of the control of some metabolite concentrations, and the extension of the multivariable control problem to higher dimensions.

Acknowledgements

The authors gratefully acknowledge the support of the FEDER program 2007-2013, in the framework of Hainaut-Biomed, and the research project OCPAM. This paper presents research results of the Belgian Network DYSCO (Dynamical Systems, Control, and Optimization), funded by the Interuniversity Attraction Poles Programme, initiated by the Belgian State, Science Policy Office. The scientific responsibility rests with its author(s).

References

[1] R.P. Nolan and K. Lee, Dynamic model of CHO cell metabolism, Metabolic Engineering 3 108–124 (2011)

[2] P. Chiarella and V.M. Fazio, Mouse monoclonal antibodies in biological research: strategies for high-throughput production, Biotechnol Lett 30 1303–1310 (2008)

[3] C. Altamirano, C. Paredes, J.J. Cairo and F. Godia, Improvement of CHO Cell Culture Medium Formulation: Simultaneous Substitution of Glucose and Glutamine, Biotechnol. Prog. 16 69–75 (2000)

[4] M. Harris, Market-Leading Biotechnology Drugs 2009: Blockbuster Dynamics in an Ailing Economy, BioWorld, Atlanta, GA, (2009)

[5] E. Jain and A. Kumar, Upstream processes in antibody production: Evaluation of critical parameters, Biotechnol Advances 26 46–72 (2008)

[6] K. Komolpis, C. Udomchokmongkol, S. Phutong and T. Palaga, Comparative production of a monoclonal antibody specific for enrofloxacin in a stirred-tank bioreactor, Journal of Industrial and Engineering Chemistry 16 567–571 (2010)

[7] G.G. Banik and C.A. Heath, Partial and total cell retention in a filtration base homogeneous perfusion reactor, Biotechnol. Prog. 11 584–588 (1995)

[8] M. Dalm, S. Cuijten, W. van Grunsven, J. Tramper and D. Martens, Effect of feed and bleed rate on hybridoma cells in an acoustic perfusion bioreactor: Part 1. Cell density, viability and cell-cycle distribution, Biotechnol. Bioeng. 88 547–557 (2004)

[9] S. Mercille, M. Johnson, S. Lanthier, A.A. Kamen and B. Massie, Understanding factors that limit the productivity of suspension-based perfusion cultures operated at high medium renewal rates, Biotechnol. Bioeng. 67 435–449 (2000)

[10] J.D. Yang, Y. Angelillo, M. Chaudhry, C. Goldenberg and D.M. Goldenberg, Achievment of high cell density and high antibody productivity by a controlled-fed perfusion bioreactor process, Biotechnol. Bioeng. 69 74–82 (2000)

[11] S.S. Ozturk, J.C. Thrift, J.D. Blackie and D. Naveh, Real-time monitoring and control of glucose and lactate concentrations in a mammalian cell perfusion reactor, Biotechnol. Bioeng. 53 372–378 (1997)

[12] J-S. Deschênes, A. Desbiens, M. Perrier and A. Kamen, Use of cell bleed in a high cell density perfusion culture and multivariable control of biomass and metabolite concentrations, Asia-Pac. J. Chem. Eng 1 82–91 (2006)

[13] J-S. Deschênes, A. Desbiens, M. Perrier and A. Kamen, Multivariable non-linear control of biomass and metabolite concentrations in a high-cell-density perfusion bioreactor, Ind. Eng. Chem. Res. 45 8985–8997 (2006)

[14] T. Zheng (ed.), Model Predictive Control, Sciyo, Rijeka (2010)

[15] E.F. Camacho and C. Bordons, Model Predictive Control, Springer-Verlag, London (2004)

[16] R. Findeisen, F. Allgöwer and L.T. Biegler, Assessment and future directions of NMPC. Berlin: Springer (2007)

[17] R.M.C. De Keyser, Model based predictive control, Invited Chapter in UNESCO Encyclopedia of Life Support Systems (EoLSS), article 6.43.16.1, vol. 83. Eolss Publishers Co Ltd, Oxford, (2003)

[18] M. de Tremblay, M. Perrier, C. Chavarie and J. Archambault, Optimization of fed-batch culture of hybridoma cells using dynamic programming: single and multi feed cases, Bioprocess Engineering 7 229–234 (1992)

[19] G. Bastin and D. Dochain, On-line Estimation and Adaptive Control of Bioreactors, Elsevier, Amsterdam (1990)

[20] E.I.P. Volcke, M. Sbarciog, E.J.L. Noldus, B. De Baets and M. Loccufier, Steady state multiplicity of two-step biological conversion systems with general kinetics, Math. Biosciences 228 160–170 (2010)

[21] A. Dhooge, W. Govaerts and Y.A. Kuznetsov, Matcont: A Matlab package for numerical bifurcation analysis of ODEs, ACM Trans. Math. Software 29 141-164 (2003)

[22] J.E. Dowd, K.E. Kwok and J.M. Piret, Glucose-based optimization of CHO-cell perfusion cultures, Biotechnol. Bioeng. 75 252-256 (2001)